

UHECR observations and lensing in the magnetic field of the Virgo cluster

K. Dolag¹, M. Kachelrieß² and D. V. Semikoz^{3,4}

¹ Max-Planck-Institut für Astrophysik, P.O. Box 1317, D-85741 Garching, Germany

² Institutt for fysikk, NTNU, N-7491 Trondheim, Norway

³ APC, 10, rue Alice Domon et Leonie Duquet, F-75205 Paris Cedex 13, France

⁴ INR RAS, 60th October Anniversary prospect 7a, 117312 Moscow, Russia

Abstract. We discuss how lensing by magnetic fields in galaxy clusters affects ultrahigh energy cosmic ray (UHECR) observations. As specific example, we use Virgo together with the cluster magnetic fields obtained earlier in a constrained simulation of structure formation including MHD processes. We find that, if M87 is the single source of UHECRs from Virgo, the emitted flux is strongly anisotropic in the most interesting energy range, (50–100) EeV, and differs from the average value by a factor five or more for a significant fraction of observers. Since magnetic lensing is energy dependent, the external energy spectrum as seen by different observers varies strongly too. These anisotropies are averaged out in the case that all active galactic nuclei in Virgo emit UHECRs. In both cases, the anisotropies of the emitted UHECR flux may introduce an important bias in the interpretation of UHECR data like, e.g., the determination of the source density n_s and the source energy spectrum of UHECRs.

PACS numbers: 98.70.Sa, 98.62.En, 98.54.Cm

1. Introduction

The identification of the sources of ultrahigh energy cosmic rays (UHECRs) is one of the most longstanding problems of astrophysics. Only recently, evidence has been accumulating that we are at the dawn of “charged particle astronomy.” A first piece of evidence have been the observation of the Greisen-Zatsepin-Kuzmin cutoff [1] in the UHECR spectrum with 5σ significance by the HiRes experiment [2] which was recently confirmed by the AUGER experiment with 6σ significance [3]. Secondly, anisotropies on medium scales have been found previously combining all available data of “old” CR experiments [4]. The data from the Pierre Auger Observatory (AUGER) presented in Ref. [5] confirmed these findings, showing also a surplus of clustering compared to an isotropic distribution in the broad range from 7 to 30 degrees. Such anisotropies were predicted as a consequence of the observed large-scale structure of matter [6] and favor therefore together with the presence of the Greisen-Zatsepin-Kuzmin cutoff the extragalactic origin of UHECRs. Comparing the expected angular auto-correlation function of different sources with the data, the authors of Ref. [7] suggested that the

sources of UHECRs are active galactic nuclei (AGN) or another strongly clustered subsample of galaxies. Finally, the Auger collaboration reported evidence for an anisotropy of the UHECR arrival directions, observing a correlation of the arrival directions of UHECRs with the positions of AGN or similarly clustered matter in the nearby Universe [8]. At present the significance of this correlation is only at the 3σ confidence level and is not confirmed by the data from the HiRes experiment [9].

Most (auto-) correlation analyses assume identical sources, emitting isotropically UHECRs. Here we show that these assumptions are not fulfilled in the case that UHECR sources are located inside regions with relatively strong magnetic fields as in the core of galaxy clusters. As a concrete example we use the Virgo cluster and investigate how lensing effects of magnetic fields extending on cluster scales influence the emitted flux and energy spectrum both for isotropic and jet-like emission of single sources. After a brief discussion of cluster magnetic fields in Sec. 2, we examine in Sec. 3 first the anisotropies in the case of a single isotropic source, then of jet-like emission by a single source, of several isotropic sources and finally the resulting modifications of the observed CR energy spectrum. We conclude in Sec. 4.

2. Magnetic fields in galaxy clusters

Magnetic fields have been detected in galaxy clusters by radio observations, via the Faraday rotation signal of the magnetized cluster atmosphere towards polarized radio sources in or behind clusters [10] and from diffuse synchrotron emission of the cluster atmosphere (see Ref. [11, 12] for recent reviews). Although our understanding of their origin is still limited, at present, numerical simulations which follow the amplification of weak magnetic seed fields by structure formation lead to a consistent picture of the predicted magnetic field and its structure within galaxy clusters [13, 14, 16, 17], well in line with the observed Faraday rotation signal. It is worth mentioning that the predicted magnetic field structure within galaxy clusters is found to not depend on details within the structures of the magnetic seed fields and therefore can be assumed to be independent on the exact mechanism which creates the magnetic seed field at high redshift [13, 15].

To obtain the predicted magnetic field structure for the Virgo cluster we used the results from a constrained realization of the local universe (see [14] and references therein). In short, the initial conditions are similar to those used by Ref. [18] in their study of structure formation in the local universe. The initial density fluctuations were constructed from the IRAS 1.2-Jy galaxy survey by smoothing the observed galaxy density field on a scale of 7 Mpc, evolving it linearly back in time, and then using it as a Gaussian constraint [19] for an otherwise random realization of the Λ CDM cosmology. The volume constrained by the IRAS observations covers a sphere of radius ≈ 115 Mpc centered on the Milky Way and therefore encloses the prominent local structure including the Virgo cluster. This region is sampled with high resolution dark matter particles and is embedded in a periodic box of around 343 Mpc length. The region outside the

constrained volume is filled with low resolution dark matter particles, allowing a good coverage of long range gravitational tidal forces. Many of the most prominent clusters observed locally can therefore be identified directly with halos in the simulation, and their positions and masses agree well with their simulated counterparts. For performing the MHD simulations, the original high resolution dark matter particles were split into gas and dark matter particles with masses of $0.69 \times 10^9 M_\odot$ and $4.4 \times 10^9 M_\odot$, respectively. The gravitational force resolution (i.e. the comoving softening length) of the simulations was set to be 10 kpc, which is comparable to the inter-particle separation reached by the SPH particles in the dense centers of our simulated galaxy clusters.

For this work we used the magnetic field configuration obtained from two realizations (MHDy and MHDz) starting from different initial seed fields (for more details see Ref. [14]) having lower (MHDy) and higher (MHDz) initial values for the magnetic seed field. Both simulations lead to magnetic fields within the galaxy clusters which are statistical in agreement with the still rare Faraday rotation measures and are roughly bracketing the allowed range of magnetic fields in galaxy clusters.

3. Anisotropies induced by cluster fields

We consider first the case that only a relatively small subset of all AGN, i.e. of order 1–10%, can accelerate to the highest energies, $E \gtrsim 10^{20}$ eV. In particular, the number density of sources is then so small that in most clusters only one UHECR source is active. A concrete example for this situation is the acceleration of UHECRs in hot spots of radio galaxies [20]. For instance, there are only few radio galaxies inside the sphere with radius 70 Mpc used in the Auger analysis [8]. The two closest radio galaxies are Centaurus A and M87. The latter AGN sits in the center of the Virgo cluster.

For the calculation of CR trajectories we use magnetic fields from the two MHD simulations of Ref. [14]. In these simulations, the magnetic field strength decreases fast for increasing distance from the cluster core, from $\text{few} \times 10^{-7}$ G at the core over $\sim 10^{-9}$ G at 0.5 Mpc to 10^{-11} G at few Mpc. We use therefore a box of size 5 Mpc centered at the position of M87 and calculate the CR trajectories under the influence of the Lorentz force until the particles leave the box. Then we prolong the trajectory to obtain the final position on a sphere with radius $d = 18$ Mpc equal to the distance to the Earth, assuming that deflections outside the box can be neglected. This implies in particular that our results do not account for the effects of the Galactic magnetic field. We consider as two main cases first the isotropic emission of UHECRs and second jet-like emission.

Before we discuss our results, we note that large deflections close to the source are not excluded by the Auger correlation signal. Since the extragalactic magnetic fields found in the simulations [14] are strongly concentrated in the core of the galaxy clusters on scales of size $l \sim 0.5$ Mpc, large deviations between the emission and exit direction from the cluster lead only to observed deflections $\vartheta \sim l/d$ of few degrees or less at the distance $d = 18$ Mpc to the Virgo cluster. More precisely, we find that the apparent size of a point source at the center of the Virgo cluster increases from 0.3° at 100 EeV

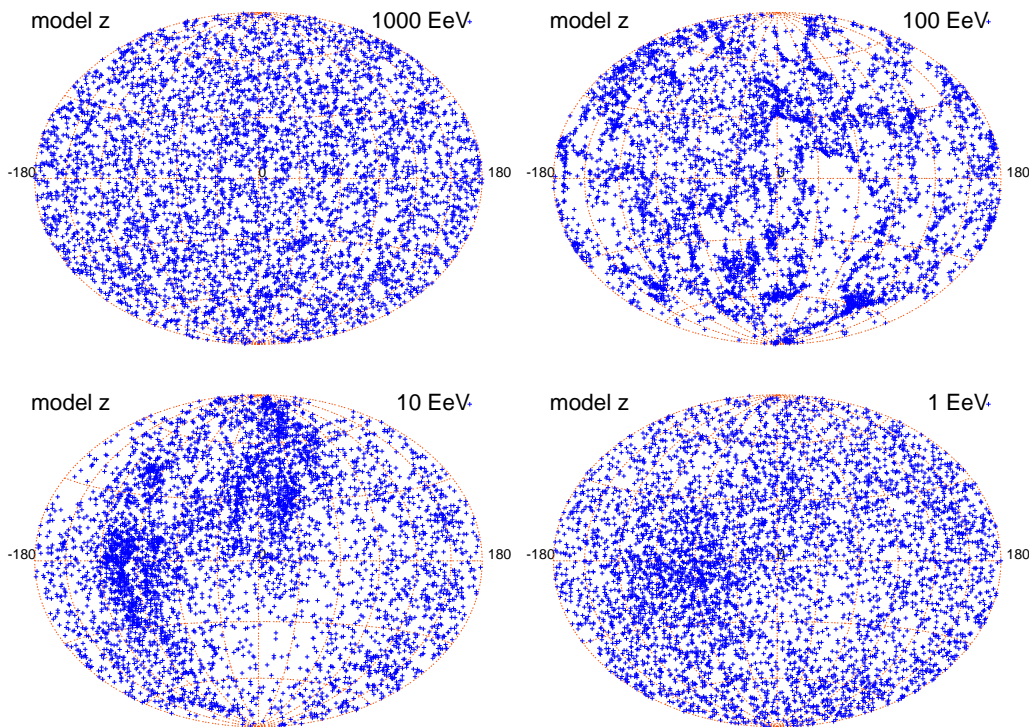


Figure 1. Skymaps of UHECR protons emitted uniformly from M87 with energies $E = 1000$ (top, left) 100, 10, and 1 EeV (lower right panel).

over 1.4° at 10 EeV to 3.6° at 1 EeV for an average observer, with sizeable deviations depending on the chosen direction.

3.1. Isotropic emission of a single source

We inject a large number of CRs with fixed energy E at the position of M87, choosing their initial propagation direction isotropically. Then we propagate each CR until it leaves a sphere of radius $R = 2.5$ Mpc around M87. We neglect all energy losses during the propagation, focusing only on the deflections due to the magnetic field. This is justified, because the average path-length in the box is even for iron at $E = 10$ EeV only 17 Mpc. Skymaps of the exit directions from this sphere are shown in Fig. 1 for protons with four different energies, $E = 1000$ EeV (upper left panel), 100 EeV, 10 EeV, and 1 EeV (lower right panel), using the simulation with stronger magnetic fields (MHDz). Large anisotropies are clearly visible by eye in the most interesting energy range, (10–100) EeV.

To quantify the probability to observe a flux modified by magnetic lensing we use the following procedure: For any random exit directions around M87 we define small areas of size $A \approx \pi\delta^2$ and calculate the number N_i of CRs per area and the average value $\langle N \rangle$. Then we count the fraction $f(\varepsilon)$ of areas where the relative number $N_i/\langle N \rangle$ of CRs is below or above a certain threshold value ε . The function $f(\varepsilon)$ depends on the chosen resolution δ , i.e. on the size $A = \pi\delta^2$ of the areas used for averaging, $f_\delta(\varepsilon)$.

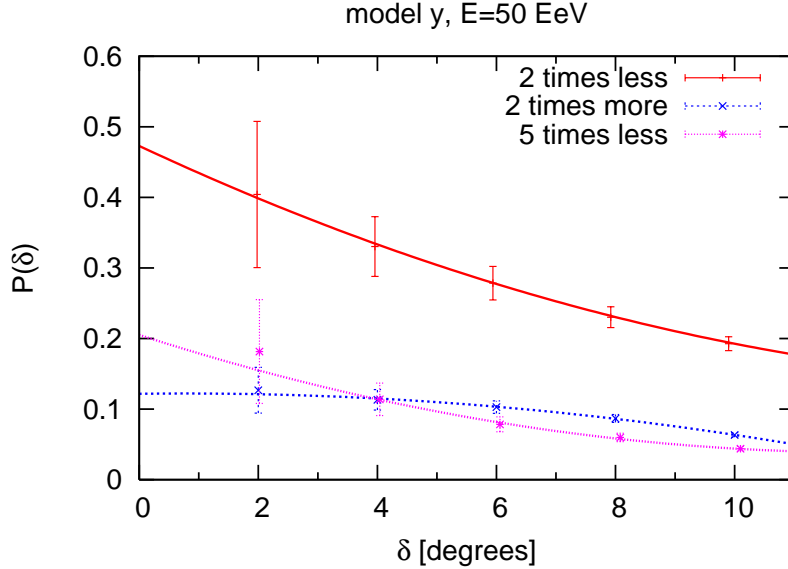


Figure 2. The fraction of regions with flux above or below a certain threshold value for several different viewing angles δ together with the extrapolation curves to $\delta \rightarrow 0$; Red, solid line is for regions with flux twice smaller, blue dashed line for twice larger and magenta dotted line for five times smaller flux than average.

A CR experiment collects during the course of a year CRs from Virgo within an opening angle $\vartheta \approx 2\text{AU}/18\text{Mpc} \approx 10^{-13}$ on a sphere centered in Virgo and radius 18 Mpc. We calculate therefore $f_\delta(\varepsilon)$ for various values of δ and extrapolate then to $\delta \rightarrow 0$. This requires a large enough total number of cosmic rays, so that all N_i are sufficiently high. For fixed δ , ε and energy E , both the value of $f_\delta(\varepsilon)$ and its uncertainty depend on the number of MC simulations. In order to extrapolate $\delta \rightarrow 0$, we need to know not only $f_\delta(\varepsilon)$, but also its fluctuations due to the finite number of MC simulations. In order to reduce the computing time, we approximate the error as $df = dN/N_{tot} = f/\sqrt{N_i}$. By performing many MC simulations for several energies we checked that this approximation for df is a factor 2 or less within the exact one.

An example for the extrapolation procedure $\delta \rightarrow 0$ is shown in Fig. 2, where the probability to observe a flux two times smaller (solid line), two times larger (dashed line) and five times smaller (dotted line) than the average flux is shown for model MHDy and $E = 50 \text{ EeV}$ for five different values of the areas $A \approx \pi\delta^2$. The errorbars show the error due to the finite number of MC simulations as discussed above. Fitting a second order polynomial $a + b\delta + c\delta^2$ to these values, we obtain finally the asymptotic value of $f_\delta(\varepsilon) = a$ for $\delta \rightarrow 0$ from a χ^2 fit.

The results for $f(\varepsilon)$ obtained in this way using the two different magnetic fields are shown in Fig. 3. Although the strength of the magnetic field at the cluster center and the deflection of individual CR trajectories differs considerably between the two simulations, the anisotropy of the emitted CR flux is very similar, in particular at low energies. The reason for this result becomes clear if one follows individual CR trajectories: The main

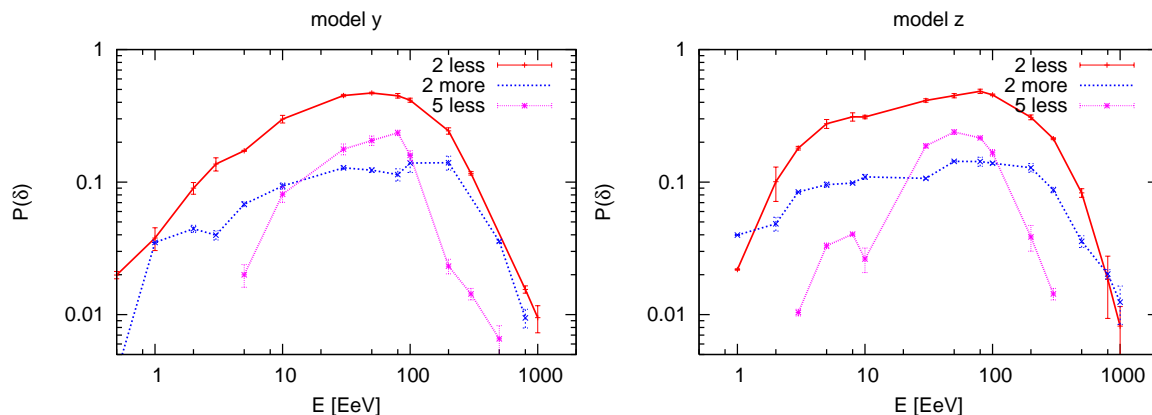


Figure 3. The fraction of sky $f(\varepsilon)$ exceeding the indicated level of anisotropy, for different energies and for magnetic fields from MHDy (left) and MHDz (right panel).

part of the deflections is caused by the extended field outside the cluster core, that has roughly the same strength in both simulations.

We discuss now the results obtained for different energies. For $E = 1000$ EeV protons propagate in the ballistic regime and deflections are small. As a result, the sky map of the emitted CR flux shown in the upper left panel of Fig. 1 is essentially isotropic, while the fraction of sky with a flux modulated by a factor two is only on the 1% level. The situation is already qualitatively different at the for us most interesting energy, $E = 100$ EeV. Deflections become sizable and regions with clearly reduced or enhanced flux are visible on the sky map, cf. the second panel of Fig. 1. The CR flux is lower than average by a factor two in 30% and by a factor 5 in 5% of the sky.

At $E = 10$ EeV protons start to propagate in the quasi-diffusive regime, and the anisotropies are weaker. However, broad over- and underdense regions are still visible in Fig. 1. By contrast, at $E = 1$ EeV protons propagate in the truly diffusive regime and most anisotropies caused by the magnetic field component are washed out: Anisotropies on a level of a factor two occur still in 4% of the sky, while stronger anisotropies have such a small probability that we could not determine them reliably ($f < 10^{-3}$).

The expected anisotropies for the case of iron (charge $Q = 26$) or other nuclei can be read off from Fig. 3 by the appropriate rescaling of their energy, $E \rightarrow E/Q$. Thus strong anisotropies, e.g. larger than a factor five, are already unlikely for iron nuclei with $E = 100$ EeV and cluster magnetic fields of the strength as typically predicted by the simulations of Ref. [14]. On the other hand, the CR flux is also for iron nuclei modulated by a factor of two in a large fraction of the sky.

We conclude that if M87 is the single source emitting UHECR in the Virgo cluster, then the emission as seen from outside of the cluster is rather anisotropic in the most interesting energy region both for iron and proton primaries. For a significant fraction of observers the flux differs from the average value by a factor five (protons) or two (iron), respectively. Hence, in models assuming that only a small fraction of all AGNs can accelerate UHECR it would be natural to observe no UHECRs from a certain fraction

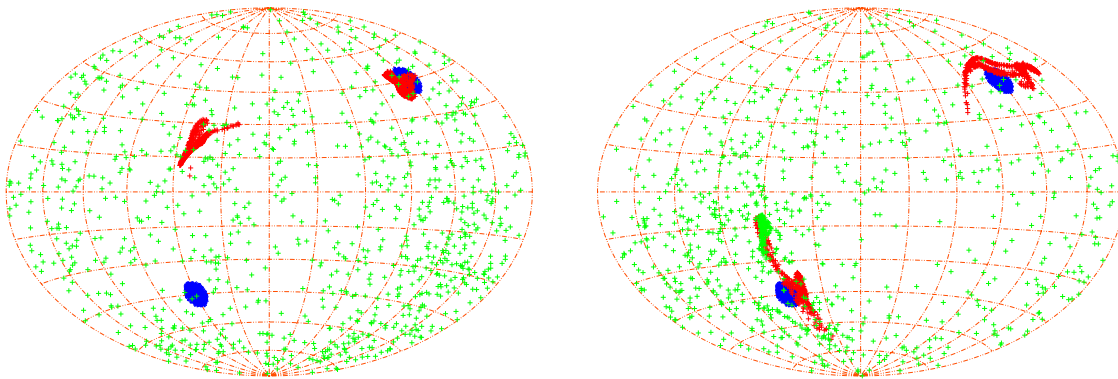


Figure 4. Skymap of UHECRs emitted in two beams (jet-like emission) from M87 with energy 60 EeV, red for protons and green for iron. The original directions are blue, the left panel uses the magnetic field from the MHDy and the right from the MHDz simulation.

of galaxy clusters, as long as the total number of UHECR observed is as small as at present. In particular, it would be no contradiction to the AGN source hypothesis that no UHECRs from the Virgo cluster have been observed with the present statistics.

3.2. Jet-like emission of a single source

We consider now the case that the acceleration of cosmic rays results in the beamed, jet-like emission of UHECRs [21]. While in the previous case of isotropic emission the magnetic field created anisotropies, its effects is now opposite, washing out the strong initial anisotropy. We compare again the results obtained for two different magnetic field models from Ref. [14], in the left and the right panels of Fig. 4. Each panel shows two jets with initial opening angle 5° in blue as well as the deflected exit directions in red for protons and in green for iron, both with $E = 60$ EeV. Both the direction and the magnitude of the deflection varies between the two simulations and different sky regions. However, both simulations agree that for the energy region relevant for UHECR astronomy, $E \gtrsim E_{\text{GZK}} \approx 50$ EeV, the solid angle Ω_{eff} of significant UHECR emission is increased by not more than a factor two for protons, while the beaming of iron nuclei is destroyed nearly completely, cf. Fig. 4. Hence beaming will decrease the effective number density of iron sources only marginally, while this effect is prominent for proton sources.

Since the clustering properties of the UHECR arrival directions [7, 25] and the correlation analysis [8] of the Auger collaboration, taken at face value, favour that the fraction of all AGN visible to us is large, the possibility that only a small subset of all AGN like radio galaxies emits narrow proton beams is strongly disfavoured.

3.3. Many sources per cluster

We assume now that all AGN emit UHECR and chose from the 12th VCV catalogue [22] all AGN closer than 2.5 Mpc to M87 as sources. Within this distance there are 13 additional AGN and many of them are outside the core of the Virgo cluster in regions with low magnetic fields. Moreover, the distance between the AGNs is much larger than the correlation length of the field and therefore the over- and underdense regions produced by different AGNs are un-correlated. Consequently, the anisotropies are drastically reduced compared to the single source case.

Assuming that all AGN have the same luminosity, we obtain a very uniform distribution of outgoing UHECR in the case of protons primaries: In less than 1% of all the sky the flux deviates more than a factor two from the average flux of UHECR protons with $E = 100$ EeV. Using iron nuclei with the same energy increases slightly the anisotropies: The iron flux is changed by a factor 2 in around 4% all of areas. We stress however that anisotropies induced by magnetic lensing for single sources lead to an important bias in studies of the density of UHECR sources and their energy spectrum, although the flux emitted by the total cluster is rather isotropic.

3.4. Modified external CR energy spectra

Since the (de-) magnification of the CR flux by magnetic fields is energy dependent, the anisotropies observed in the previous subsections lead to a modulation of the initial CR spectrum for an outside observer. In the Fig. 5 we show the energy spectrum dN/dE as function of energy for 10^6 CRs and three different regions of size $\delta = 8^\circ$ in the top panels, while skymaps of 5000 UHECR protons emitted with an energy spectrum $dN/dE \propto E^{-2.2}$ and threshold energy $E > E_0 = 5$ EeV are shown in the bottom. We assume first that only one source, M87, emits UHECRs. For both models MHDy (left) and MHDz (right) we show the original spectrum in red, in a region with average flux (blue crosses), and in two regions with increased (green boxes) and reduced (magenta circles) flux, respectively. In all cases, the spectrum is larger or smaller than average for several nearby bins. This mean that lensing effects are not washed out by the finite experimental energy resolution. Also the statistical errors shown in Fig. 5 are small enough not to affect the conclusions above. Thus, magnetic lensing does not only change the value of the UHECR flux in a given direction, but also changes its energy dependence: Depending on the threshold energy and the direction considered, the exponent of the estimated power-law $dN/dE \propto E^{-\alpha}$ may differ strongly. Note that the shown energy spectrum will be additionally modified both by propagation effects and by the Galactic magnetic field. The latter will not only deflect CRs but will lead additionally to a similar modulation of the CR energy spectra as the cluster field.

Next we investigate how fast this modification of the CR spectrum disappears, if the the number of sources increases. In Fig. 6, we show again the energy spectrum for two regions with reduced (left) and increased (right) flux, varying now the number of sources. While in the case of a spot with small anisotropy the modified energy spectrum resembles

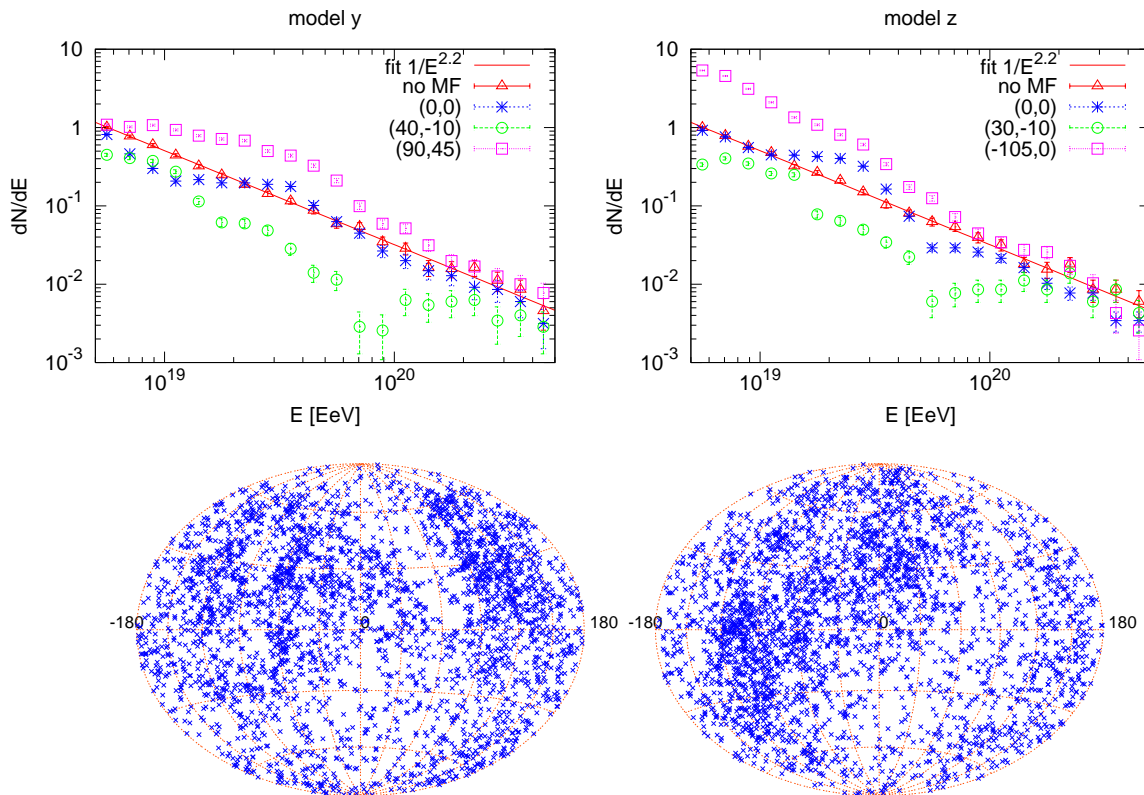


Figure 5. The energy spectrum dN/dE as function of energy (top) and skymaps of UHECR protons emitted uniformly from M87 (bottom) for models MHDy (left) and MHDz (right). The energy spectrum is shown for $\delta = 8^\circ$ regions and 10^6 events over the sky for the following cases: in absence of magnetic field (red), spectrum in overdense region (magenta), underdense region (green) and ordinary region (blue).

already for two sources the original one, the modification of the energy spectrum in case of a large anisotropy is non-negligible even if all 14 AGN contribute equally to the flux. Finally, we remark that the case with 14 sources with equal luminosity is rather unrealistic, since the large difference in (bolometric) luminosity between M87 and the other AGN in the Virgo cluster should be reflected also in their UHECR luminosity.

4. Conclusions

The amplification of the UHECR flux by magnetic lensing was discussed previously in the context of the Galactic regular and turbulent field [23, 24]. For instance, Ref. [24] calculated exposure maps for three different models of the Galactic regular magnetic field and found also significant anisotropies at $E = 40$ EeV. The strength of the magnetic field close to the core of galaxy clusters is smaller by a factor 30–100 than in the Milky Way. The weakness of cluster fields is, however, over-compensated by their much larger extension compared to the Galactic disc. While the deflection of UHECRs in cluster fields leads even for the nearest cluster only to maximal angular differences

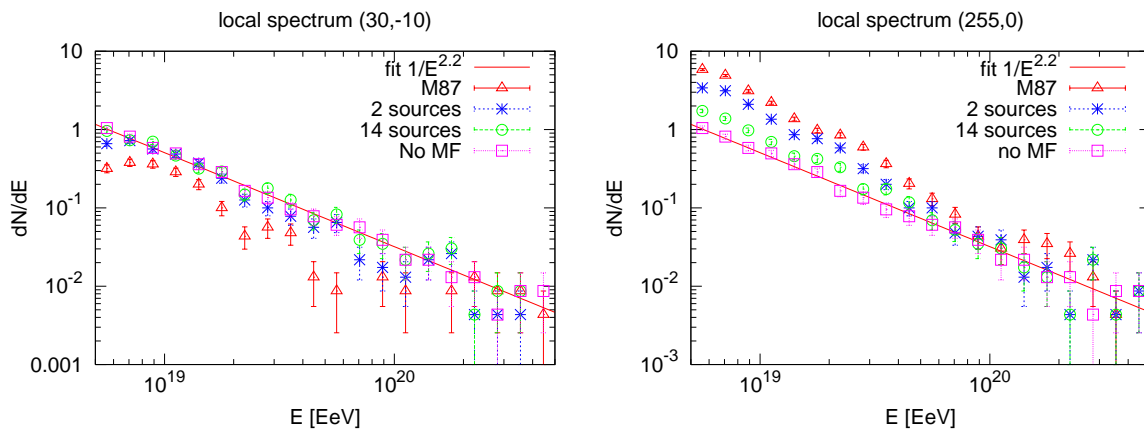


Figure 6. The energy spectrum dN/dE as function of energy for model MHDz and a varying number of sources; left for underdense and right for an overdense region.

between the source and the arrival direction of order 1.5° and is thus negligible, the resulting anisotropies of the emitted CR flux may introduce an important bias in the interpretation of CR data.

We have found that assuming magnetic fields as in Ref. [14] the flux from M87 differs from the average value by a factor five for a significant fraction of observers in the most interesting energy region, (50–100) EeV. This may be the explanation for the non-observation of UHECR from the Virgo cluster, if M87 is the dominant UHECR source in the Virgo cluster. More generally, anisotropies induced by magnetic fields result in a reduction of the effective number of sources, leading to a bias in auto-correlation studies. Vice versa, if the source type of UHECRs and thus their number density is known, a comparison with the estimated value from auto-correlation studies informs us about the importance of anisotropies and/or beaming effects. Note that magnetic lensing will affect also sources behind the Virgo cluster.

The second important consequence of the anisotropies induced by the cluster magnetic fields is the resulting modulation of the energy spectrum of UHECRs leaving the galaxy cluster compared to their generation spectrum. A similar energy modulation is be introduced by the Galactic magnetic field and both effects will complicate the reconstruction of generation spectrum, if UHECRs sources are discovered.

Finally we want to stress that we obtained all our results for two specific realizations of magnetic fields obtained within the simulations of Ref. [14]. Although we expect that the main features of our results are robust, quantitative differences will appear using different simulations of cluster magnetic fields: For instance, if the volume fraction filled by relatively large magnetic fields around clusters is as large as in Ref. [26], we expect that the same phenomena happen as found in this work, but extending over a larger energy range.

Acknowledgments

M.K. would like to thank the Max-Planck-Institut für Physik in Munich for hospitality and support.

References

- [1] K. Greisen, “End To The Cosmic Ray Spectrum?,” *Phys. Rev. Lett.* **16**, 748 (1966); G. T. Zatsepin and V. A. Kuzmin, “Upper Limit Of The Spectrum Of Cosmic Rays,” *JETP Lett.* **4**, 78 (1966) [*Pisma Zh. Eksp. Teor. Fiz.* **4**, 114 (1966)].
- [2] R. Abbasi *et al.* [HiRes Collaboration], *Phys. Rev. Lett.* **100**, 101101 (2008) [arXiv:astro-ph/0703099].
- [3] Pierre Auger Collaboration, “Observation of the suppression of the flux of cosmic rays above 4×10^{19} eV,” arXiv:0806.4302 [astro-ph].
- [4] M. Kachelrieß and D. V. Semikoz, “Clustering of ultra-high energy cosmic ray arrival directions on medium scales,” *Astropart. Phys.* **26**, 10 (2006) [astro-ph/0512498].
- [5] S. Mollerach *et al.*, for the Pierre Auger Collaboration, “Studies of clustering in the arrival directions of cosmic rays detected at the Pierre Auger Observatory above 10 EeV,” to appear in *Proc. “30th International Cosmic Ray Conference”, Mérida, Mexico, 2007*, arXiv:0706.1749 [astro-ph].
- [6] T. Stanev *et al.*, “The Arrival directions of the most energetic cosmic rays,” *Phys. Rev. Lett.* **75**, 3056 (1995) [astro-ph/9505093]. E. Waxman, K. B. Fisher and T. Piran, “The signature of a correlation between $> 10^{19}$ eV cosmic ray sources and large scale structure,” *Astrophys. J.* **483**, 1 (1997) [astro-ph/9604005]. A. Smialkowski, M. Giller and W. Michalak, “Luminous infrared galaxies as possible sources of the UHE cosmic rays,” *J. Phys. G* **28**, 1359 (2002) [astro-ph/0203337]. G. Sigl, F. Miniati and T. A. Ensslin, “Ultra-high energy cosmic rays in a structured and magnetized universe,” *Phys. Rev. D* **68**, 043002 (2003) [astro-ph/0302388]. A. Cuoco, G. Miele and P. D. Serpico, “First hints of large scale structures in the ultra-high energy sky?,” *Phys. Rev. D* **74**, 123008 (2006) [astro-ph/0610374]; “Astrophysical interpretation of the medium scale clustering in the ultra-high energy sky,” *Phys. Lett. B* **660**, 307 (2008) [astro-ph/0706.2864].
- [7] A. Cuoco *et al.*, “Clustering properties of ultrahigh energy cosmic rays and the search for their astrophysical sources,” *Astrophys. J.* **676**, 807 (2008) [astro-ph/0709.2712]; “A global autocorrelation analysis of the Auger data,” arXiv:0809.4003 [astro-ph].
- [8] J. Abraham *et al.* [Pierre Auger Collaboration], “Correlation of the highest energy cosmic rays with nearby extragalactic objects,” *Science* **318**, 938 (2007) [astro-ph/0711.2256], “Correlation of the highest-energy cosmic rays with the positions of nearby active galactic nuclei,” *Astropart. Phys.* **29**, 188 (2008) [astro-ph/0712.2843]; for criticism see D. Gorbunov, P. Tinyakov, I. Tkachev and S. Troitsky, “Comment on ‘Correlation of the Highest-Energy Cosmic Rays with Nearby Extragalactic Objects’,” arXiv:0711.4060 [astro-ph].
- [9] R. U. Abbasi *et al.* [HiRes Collaboration], “Search for Correlations between HiRes Stereo Events and Active Galactic Nuclei,” arXiv:0804.0382 [astro-ph].
- [10] C. L. Carilli, G. B. Taylor, “Cluster Magnetic Fields”, *Ann. Rev. Astron. Astrophys.* **40**, 319 (2002).
- [11] C. Ferrari *et al.*, “Observations of Extended Radio Emission in Clusters”, *Space Science Rev.* **134**, 93 (2008).
- [12] F. Govoni and L. Feretti, “Magnetic Fields in Clusters of Galaxies”, *Int. J. Mod. Phys. D* **13**, 1549 (2004).
- [13] K. Dolag, M. Bartelmann and H. Lesch, “SPH simulations of magnetic fields in galaxy cluster”,

- Astron. Astrophys. **348**, 351 (1999); “Evolution and structure of magnetic fields in simulated galaxy clusters”, Astron. Astrophys. **387**, 383 (2002).
- [14] K. Dolag, D. Grasso, V. Springel and I. Tkachev, “Constrained simulations of the magnetic field in the local universe and the propagation of UHECRs,” JCAP **0501**, 009 (2005) [astro-ph/0410419].
- [15] J. Donnert, K. Dolag, H. Lesch and E. Müller, “Cluster Magnetic Fields from Galactic Outflows”, arXiv:0808.0919 [astro-ph], submitted to Mon. Not. Roy. Astron. Soc.
- [16] M. Brüggen *et al.*, “Simulations of Magnetic Fields in Filaments”, Astrophys. J. Lett. **631**, L21 (2005).
- [17] Y. Dubois and R. Teyssier, “Cosmological MHD simulation of a cooling flow cluster”, Astron. Astrophys. **482**, L13 (2008).
- [18] H. Mathis *et al.*, “Simulating the formation of the local galaxy population”, MNRAS, **333**, 739 (2002).
- [19] Y. Hoffman and E. Ribak, “Constrained realizations of Gaussian fields - A simple algorithm”, Astrophys. J. Lett. **380**, L5 (1991).
- [20] K. Mannheim, “The Proton blazar,” Astron. Astrophys. **269**, 67 (1993) [astro-ph/9302006]. J. P. Rachen and P. L. Biermann, “Extragalactic Ultrahigh-Energy Cosmic Rays. 1. Contribution From Hot Spots In FR-II Radio Galaxies,” Astron. Astrophys. **272**, 161 (1993) [astro-ph/9301010]. J. P. Rachen, “Ultra-high energy cosmic rays from radio galaxies revisited,” arXiv:0808.0349 [astro-ph].
- [21] Y. Y. Kovalev, M. L. Lister, D. C. Homan and K. I. Kellermann, Astroph. J. Lett. **668**, L27 (2007) arXiv:0708.2695 [astro-ph].
- [22] M.-P. Véron-Cetty and P. Véron, “A catalogue of quasars and active nuclei: 12th edition,” Astron. Astroph. **455**, 773 (2006).
- [23] D. Harari, S. Mollerach and E. Roulet, “The toes of the ultra high energy cosmic ray spectrum,” JHEP **9908**, 022 (1999) [astro-ph/9906309]. D. Harari, S. Mollerach, E. Roulet and F. Sanchez, “Lensing of ultra-high energy cosmic rays in turbulent magnetic fields,” JHEP **0203**, 045 (2002) [astro-ph/0202362].
- [24] M. Kachelrieß, P. D. Serpico and M. Teshima, “The galactic magnetic field as spectrograph for ultra-high energy cosmic rays,” Astropart. Phys. **26**, 378 (2006) [astro-ph/0510444].
- [25] S. L. Dubovsky, P. G. Tinyakov and I. I. Tkachev, “Statistics of clustering of ultra-high energy cosmic rays and the number of their sources,” Phys. Rev. Lett. **85**, 1154 (2000) [astro-ph/0001317]; S. Fodor and S. D. Katz, “Ultra high energy cosmic rays from compact sources,” Phys. Rev. D **63**, 023002 (2001) [hep-ph/0007158]; P. Blasi and D. De Marco, “The small scale anisotropies, the spectrum and the sources of ultra high energy cosmic rays,” Astropart. Phys. **20**, 559 (2004) [astro-ph/0307067]; M. Kachelrieß and D. Semikoz, “Ultra-high energy cosmic rays from a finite number of point sources,” Astropart. Phys. **23**, 486 (2005) [astro-ph/0405258].
- [26] G. Sigl, F. Miniati and T. A. Enßlin, “Ultra-high energy cosmic ray probes of large scale structure and magnetic fields,” Phys. Rev. D **70**, 043007 (2004) [astro-ph/0401084].